Exploiting a ^{13}C-labelled heparin analogue for *in situ* solid-state NMR investigations of peptide-glycan interactions within amyloid fibrils

Jillian Madine, Jonathan C. Clayton, Edwin A. Yates and David A. Middleton

Received 20th November 2008, Accepted 25th February 2009
First published as an Advance Article on the web 31st March 2009
DOI: 10.1039/b820808e

Pathological amyloid deposits are mixtures of polypeptides and non-proteinaceous species including heparan sulfate proteoglycans and glycosaminoglycans (GAGs). We describe a procedure in which a ^{13}C-labelled N-acetyl derivative of the GAG heparin ([^{13}C-CH_3]NAcHep) serves as a useful probe for the analysis of GAG-protein interactions in amyloid using solid-state nuclear magnetic resonance (SSNMR) spectroscopy. NAcHep emulates heparin by enhancing aggregation and altering the fibril morphology of $A\beta_{1-40}$, one of the β-amyloid polypeptides associated with Alzheimer's disease, and α-synuclein, the major protein component of Lewy bodies associated with Parkinson's disease. ^{13}C SSNMR spectra confirm the presence of [^{13}C-CH_3]NAcHep in $A\beta_{1-40}$ fibril deposits and detect dipolar couplings between the glycan and arginine R_5 at the $A\beta_{1-40}$ N-terminus, suggesting that the two species are intimately mixed at the molecular level. This procedure provides a foundation for further extensive investigations of polypeptide-glycan interactions within amyloid fibrils.

Introduction

The term amyloid was attributed, over 100 years ago, to the starch-like proteinaceous deposits associated with pathological lesions of the brain.[1] Amyloid has since become synonymous with the disease-associated proteins and peptides deposited extracellularly as highly ordered fibrils with a common cross-β structure giving rise to Congo red birefringence.[2] Recent insights into the molecular architecture of amyloid fibrils have been aided by advances in the techniques of X-ray crystallography and solid-state nuclear magnetic resonance (SSNMR),[3–5] the latter of which is particularly useful for characterising amyloid heterogeneity, structural polymorphism or strain behaviour.[6,7] X-Ray analysis of microcrystals of short amyloidogenic peptide segments have revealed a common cross-β spine motif formed by a minimum of two β-sheet layers,[8] which can pack together with interdigitated side-groups forming a steric zipper.[3] Structural constraints from SSNMR measurements have enabled detailed models to be proposed for several amyloid assemblies, both for intact native polypeptides and for segments thereof.[5]These include amyloid β-peptides,[4,6] amylin,[9] β_2-microglobulin,[10] transthyretin[11] and α-synuclein.[7]

Structural studies of insoluble amyloid have so far focused on aggregates of proteins in isolation under controlled conditions, but amyloid deposits associated with pathological disorders are complex mixtures of protein aggregates, nucleic acids, heparan sulfate proteoglycans (HSPGs) and glycosaminoglycans (GAGs),[12] and various other polyelectrolytes, which may have profound effects on fibril architecture.[13] There is substantial evidence that GAG groups of HSPGs play an active role in amyloid fibril formation[14–16] and recent studies suggest that synergistic action of multiple solute cofactors could play roles in amyloid-type fibrillogenesis of pathogenic polypeptides.[16] Moreover, it is known that amyloid fibril assemblies with diverse morphologies or molecular architectures can grow from the same initial polypeptide sequence, either spontaneously or promoted by specific growth conditions.[17] The amyloid plaques associated with Alzheimer's disease consist of fibrils of the 40 and 42 amino acid β-amyloid polypeptides $A\beta_{1-40}$ and $A\beta_{1-42}$ co-localised with proteoglycans.[12] HSPGs and GAGs such as heparan sulfate and heparin enhance the rate of formation of $A\beta_{1-40}$ and $A\beta_{1-42}$[18] fibrils formed *in vitro* as well as fibrils from several unrelated proteins including amylin[15,16] and prion proteins.[19] The negatively charged sulfate moieties of GAGs are critical for enhancing fibril formation[20] and may associate with clusters of basic residues occurring in these proteins. For example the N-terminus of $A\beta_{1-40}$ contains R_5, H_6 and V_{12}HHQKL, a proposed heparin binding site.[21] Heparin and the HSPG agrin also enhance the aggregation and fibril yield of the 140 amino acid protein α-synuclein, the major protein component of Lewy bodies associated with Parkinson's disease.[14,22] α-Synuclein has a repeating basic sequence at the N-terminus which could serve as a site for interaction with polyanionic species such as GAGs and HSPGs.

Studies of the interactions between polypeptide and GAGs or other non-proteinaceous species in amyloid deposits at the molecular level have so far been hampered by the lack of suitable procedures. Here with ^{13}C SSNMR analysis of a heparan sulfate (HS) analogue we demonstrate a new method for examining GAG-protein interactions *in situ* within amyloid fibrils. The HS analogue, NAcHep, was prepared by selectively removing the N-linked sulfate groups of heparin (retaining the O-linked sulfates) and replacing them with N-acetyl groups.[23,24] These simple steps provide a convenient route to incorporate an NMR probe into a GAG (in this case ^{13}C at the CH_3 position of the acetyl substituent) that gives rise to a signature peak in the ^{13}C NMR spectrum that would confirm co-localisation of the analogue with amyloid fibrils

School of Biological Sciences, University of Liverpool, Crown Street, Liverpool, L69 7ZB, United Kingdom. E-mail: middleda@liv.ac.uk; Tel: +44 (0)151 7954457

(Fig. 1). It is shown that NAcHep closely emulates the action of heparin both in enhancing the rate of $A\beta_{1-40}$ and α-synuclein (asyn) aggregation and in modifying the morphology of the mature fibrils formed by both proteins at the end-point of aggregation. Measurements of dipolar coupling between ^{13}C labelled NAcHep and selectively ^{13}C labelled $A\beta_{1-40}$ confirm that the two compounds form an intimate mixture within amyloid fibrils, thus providing incentive for further experiments to examine the interaction in greater detail.

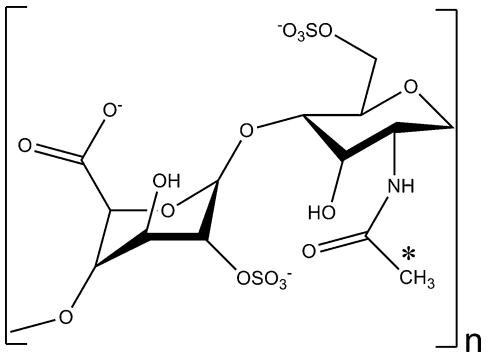

Fig. 1 The chemical structure of NAcHep.

Results

Experiments were first conducted to confirm that the NAcHep reproduces the effects of heparin on the rate of $A\beta_{1-40}$ aggregation and on the morphology of the fibrils deposited at the end-point of aggregation.

The effects of heparin and NAcHep on $A\beta_{1-40}$ aggregation

The rate of aggregation of $A\beta_{1-40}$ alone and in the presence of Hep or NAcHep was monitored with thioflavin T (ThT) fluorescence measurements, to detect the formation of amyloid, and by dynamic light scattering (DLS), to observe changes in particle size (Fig. 2). A low peptide concentration (20 μM) was examined so as to reduce the rate of aggregation and allow the effects of Hep and NAcHep to be monitored at several intervals before the insoluble aggregates are formed at the end-point. ThT binds to aggregated amyloid, causing a change in absorbance values of its excitation and emission spectra.[26] Enhancement of ThT fluorescence is consistent with an increased rate for the formation of amyloid and has previously been observed for $A\beta_{1-40}$ in the presence of intact and de-N-sulfated heparin at similar peptide concentrations.[20] Here, as little as 1 μM Hep or NAcHep was sufficient to enhance the ThT fluorescence by at least 30% at all time points investigated (Fig. 2a). At these concentrations the initial solution contains approximately one saccharide unit for each peptide molecule. Equimolar and higher (20 μM and 100 μM) concentrations of Hep and NAcHep with respect to $A\beta_{1-40}$ did not enhance ThT fluorescence further (Fig. 2b) suggesting that binding to the peptide was saturated at low GAG-peptide molar ratios. Control experiments with 100 μM Hep or NAcHep but omitting $A\beta_{1-40}$ showed no ThT fluorescence, confirming that the GAGs did not interfere with the measurements. DLS indicated that $A\beta_{1-40}$ alone formed aggregates of < 500 nm diameter after incubation for up to 1 h and much larger particles (diameter > 2000 nm) at the 4 h end-point (Fig. 2c). In the presence of Hep and NAcHep the larger particles formed within 60 min of aggregation.

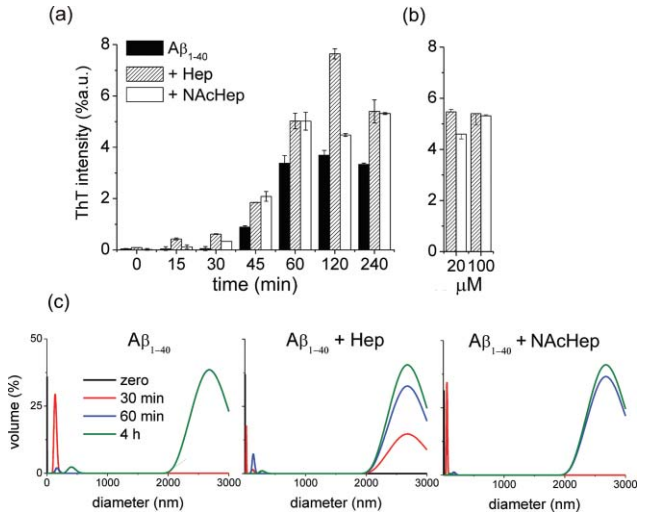

Fig. 2 Effect of Hep and NAcHep on the rates of aggregation of $A\beta_{1-40}$ at 37 °C. (a) Time dependence of amyloid formation by 20 μM $A\beta_{1-40}$ alone, with 1 μM Hep or with 1 μM NAcHep, monitored by changes in ThT fluorescence. Means and standard errors are shown for 3 samples per time point. (b) Effect of higher Hep and NAcHep concentrations on amyloid formation after 240 min, monitored by ThT fluorescence. (c) Particle sizes formed by 20 μM $A\beta_{1-40}$ alone (left), with 1 μM heparin (middle) or with 1 μM NAcHep (right), monitored by DLS at time 0 (black), 30 minutes (red), 60 minutes (blue) and 4 hours (green).

Electron microscopy (EM) was used to visualise $A\beta_{1-40}$ aggregates formed after incubation of the peptide for 24 h. The peptide alone forms a network of unbranched fibrils after incubation at a concentration of 1 mM (Fig. 3a, (i)). Incubation of $A\beta_{1-40}$ with unmodified heparin (Hep) has a marked effect on the morphology of the fibrils as they become longer and more slender than fibrils of $A\beta_{1-40}$ alone and with more branching (Fig. 3a, (ii)). This elongated morphology was also observed when $A\beta_{1-40}$ fibrils were grown in the presence of NAcHep under identical conditions (Fig. 3a, (iii)).

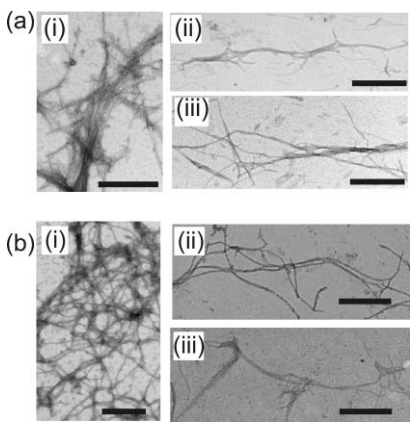

Fig. 3 Negative-stain electron micrographs showing the effects of Hep and NAcHep on the morphology of $A\beta_{1-40}$ fibrils formed after incubation for 24 h. (a) 20 μM $A\beta_{1-40}$ alone (i), in the presence of 1 μM Hep with a mean molecular mass of 16 kDa (ii) or in the presence of 1 μM NAcHep (iii). (b) 1 mM $A\beta_{1-40}$ alone (i), in the presence of 1 mM Hep (ii) or in the presence of 1 mM NAcHep (iii). Scale bar is 500 nm.

Similar wispy deposits have been isolated from mice 1 week after infusion with $A\beta_{1-40}$ and HSPG,[25] and have also been observed for α-synuclein aggregates in the presence of heparin and other GAGs.[14] Hep and NAcHep therefore have a similar effect on the final morphology of the mature fibrils. EM analysis of aggregates formed from 1 mM $A\beta_{1-40}$ with and without NAcHep at an equimolar concentration (Fig. 3b) exhibited morphologies similar to the fibrils grown from 20 μM protein and 1 mM heparin or NAcHep (Fig. 3a). This higher protein concentration was required later on in order to maximise the fibril yield for NMR sensitivity purposes.

The EM, ThT and DLS measurements therefore concur that NAcHep and Hep behave similarly in enhancing the rate of aggregation of $A\beta_{1-40}$ and in altering the morphology of the mature fibrils.

The effects of heparin and NAcHep on α-synuclein aggregation

Further experiments were carried out to assess whether NAcHep could serve as a proxy for heparin in promoting fibril growth by asyn, another protein known to interact with GAGs and HSPGs.[14,22] NAcHep and Hep behaved similarly in enhancing ThT binding to α-synuclein after incubation of the protein with the GAGs for 3 days and 7 days, consistent with an higher rate of fibril growth relative to the protein alone (Fig. 4a). DLS indicated that the protein incubated with NAcHep and Hep aggregated into larger particles at day 3 and day 7 than when incubated alone (data not shown). EM revealed that asyn alone formed a disperse assortment of slender fibrils after incubation for 7 days, but in the presence of NAcHep and Hep the protein produced a much more dense network of tangled fibrils (Fig. 4b). These experiments together demonstrate that NAcHep has a similar effect to Hep in enhancing the rate of aggregation and fibril yield of asyn.

SSNMR Detection of NAcHep in fibril deposits

In order to confirm that NAcHep co-localised with the protein in $A\beta_{1-40}$ or asyn fibrils, the procedure for preparing NAcHep was exploited to incorporate $^{13}CH_3$ N-acetyl groups into the de-N-sulfated heparin to yield [^{13}C-CH_3]NAcHep. High-resolution SSNMR could then be used to detect the characteristic signal from the labelled analogue within the fibrils. In all the NMR experiments fibrils were grown from 1 mM protein in the presence of an equimolar concentration of [^{13}C-CH_3]NAcHep.

A ^{13}C cross-polarization magic-angle spinning (CP-MAS) NMR spectrum of [^{13}C-CH_3]NAcHep alone in aqueous solution shows a single signature peak at a chemical shift of 23.5 ppm, which is the value expected from earlier solution-state NMR studies[24] (Fig. 5a). A CP-MAS NMR spectrum of unlabelled $A\beta_{1-40}$ fibrils grown with equimolar [^{13}C-CH_3]NAcHep (Fig. 5b) exhibits two peaks from [^{13}C-CH_3]NAcHep, one at 23.5 ppm and one at 18.5 ppm. The additional peak suggests that NAcHep populates different environments within the fibrils, although at this stage it is only possible to speculate on where the different sites may be. The peak at 23.5 ppm is virtually identical to that for NAcHep alone, and it is conceivable that this signal arises from a population of NAcHep that is unbound or only superficially associated with the fibrils at site(s) that are similar in character to the aqueous phase. The peak at 18.5 ppm represents a

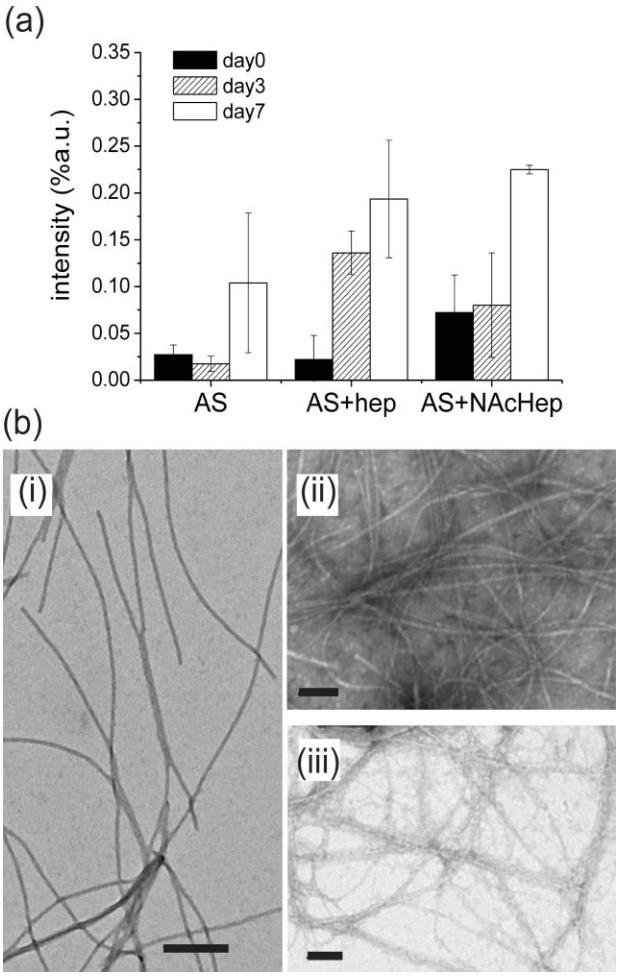

Fig. 4 Effect of Hep and NAcHep on the rates of aggregation of α-synuclein and the morphology of the fibrils. (a) Time dependence of amyloid formation by 20 μM α-synuclein alone, with 20 μM Hep or with 20 μM NAcHep, monitored by changes in ThT fluorescence. Means and standard errors are shown for 3 samples per time point. (b) Negative-stain electron micrographs show fibrils formed by 20 μM protein alone (i), in the presence of 20 μM Hep (ii) and in the presence of 20 μM NAcHep (iii). Scale bar is 200 nm.

substantial frequency shift with respect to NAcHep alone, which perhaps reflects differences in hydrogen-bonding to the acetate carbonyl, hydrophobic interactions or ring current effects, any combination of which may enhance chemical shielding at the $^{13}CH_3$. Both peaks are rather broad and consistent with structural heterogeneity or polydispersity inherent in the polysaccharide or with heterogeneity in the populations of NAcHep associated with $A\beta_{1-40}$. Interestingly, the spectrum of unlabelled asyn fibrils grown with equimolar [^{13}C-CH_3]NAcHep showed no evidence of a peak for the free glycan at 23.5 ppm and was instead dominated by a peak at close to 18.5 ppm (Fig. 5c). This peak broadened considerably at the base, again consistent with structural heterogeneity or polydispersity in the polysaccharide, in the complex or both. The apparent lack of free [^{13}C-CH_3]NAcHep suggests that the lysine-rich N-terminal region of asyn is more effective at binding and sequestering polyanionic species during aggregation than is $A\beta_{1-40}$, which is less basic overall.

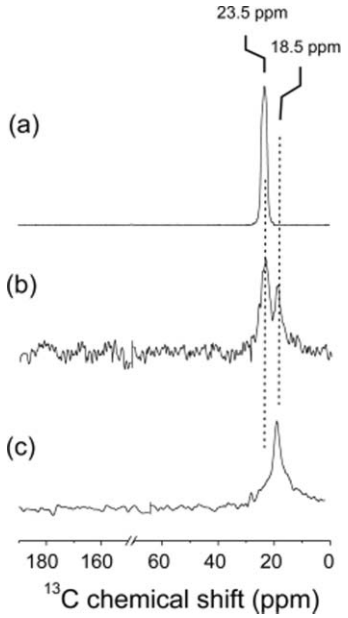

Fig. 5 Carbon-13 CP-MAS NMR experiments to identify signals for [^{13}C-CH$_3$]NAcHep. (a) Spectrum of 1 mM [^{13}C-CH$_3$]NAcHep alone in aqueous solution at −25 °C. (b) Spectrum of fibrils prepared from 1 mM unlabelled Aβ_{1-40} in the presence of 1 mM [^{13}C-CH$_3$]NAcHep. (c) Spectrum of fibrils prepared from 1 mM unlabelled α-synuclein in the presence of 1 mM [^{13}C-CH$_3$]NAcHep.

These results demonstrate that [^{13}C-CH$_3$]NAcHep is a sensitive NMR probe for detecting the association of GAGs with amyloid fibrils, which is crucial if further structural investigations of peptide-glycan interactions are to be carried out with this compound.

Interactions between NAcHep and Aβ_{1-40}

Further experiments were conducted to detect interactions between [^{13}C-CH$_3$]NAcHep and Aβ_{1-40} *in situ* within the amyloid fibrils. The aim was to establish the practical feasibility of detecting intermolecular dipolar coupling between ^{13}C labels in the saccharide and in the protein using SSNMR, which would be diagnostic of an intimate interaction between the two species. Detection of intermolecular couplings of this nature have not yet been reported for any amyloid system and so, if successful, this experiment would provide an incentive to perform more extensive measurements of multiple couplings to map the peptide-GAG binding interface in future investigations. Aβ_{1-40} was studied in preference to asyn because the former peptide is amenable to solid-phase synthesis and could be isotopically labelled at selective sites for simplicity.

To search for interactions between NAcHep and Aβ_{1-40}, fibrils were prepared from [^{13}C-CH$_3$]NAcHep and Aβ_{1-40} which was uniformly ^{13}C labelled at Arg5 ([U-^{13}C-R$_5$]Aβ_{1-40}), one of the proposed sites for GAG binding at the N-terminus of the peptide.[21] Other sites could in principle be labelled as well, but this would introduce greater complexity into the spectrum, particularly if the peaks are broad. Detection of ^{13}C-^{13}C dipolar couplings between R5 of the peptide and [^{13}C-CH$_3$]NAcHep would signify a through-space intermolecular distance of less than approximately 6 Å. Unfortunately, even with only this single residue labelled, the ^{13}C CP-MAS spectrum of the fibrils is dominated by the peaks from the peptide (Fig. 6a), which are very broad and thus consistent with the disorder that is known to occur at the N-terminus.[4] Consequently the presence of [^{13}C-CH$_3$]NAcHep in the fibrils cannot be confirmed from the CP-MAS spectrum, chiefly because the broad peaks from Cβ/Cγ of the peptide extend across the region where the peaks are expected for [^{13}C-CH$_3$]NAcHep. Although shoulders do appear at ~19 ppm and ~24 ppm, which apparently do not arise from the peptide, these could not be assigned to [^{13}C-CH$_3$]NAcHep unambiguously. It was therefore necessary to use a combination of editing and filtering experiments to positively assign signals to the labelled saccharide.

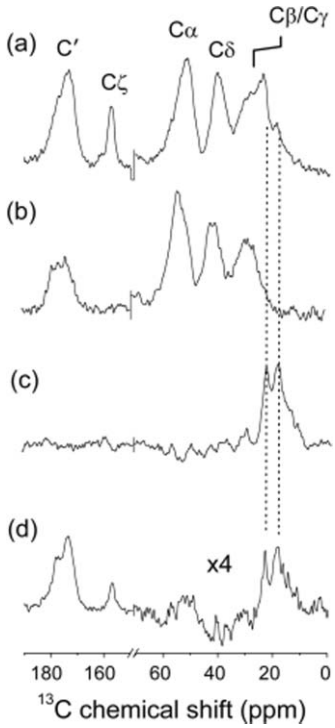

Fig. 6 Carbon-13 SSNMR experiments to confirm the presence of [^{13}C-CH$_3$]NAcHep in mixed fibrils with [U-^{13}C-R5]Aβ_{1-40}. (a) CP-MAS spectrum of fibrils prepared from 1 mM [U-^{13}C-R$_5$]Aβ_{1-40} fibrils in the presence of 1 mM [^{13}C-CH$_3$]NAcHep. Peaks are labelled with the assignments to the carbonyl carbon (C′), Cα, side-chain aliphatic carbons (Cβ, Cγ, Cδ) and guanidinium carbon (Cζ) of R5. Subsequent spectra (for the same sample) are: (b) a DQF spectrum; (c) a DRAMA spectrum; (d) a spectrum obtained with PI. Dashed lines highlight the expected peak positions (18.5 ppm and 23.5 ppm) for the two species of [^{13}C-CH$_3$]NAcHep identified in Fig. 5.

A double quantum filtered (DQF) experiment was first used to select signals only from the strongly coupled network of ^{13}C spins within the peptide and to eliminate any signals from [^{13}C-CH$_3$]NAcHep, which will be more weakly coupled (Fig. 6b). The double quantum filter eliminates the peak for the guanidinium Cζ or R5, which is bonded only to nitrogen and so is weakly coupled to other ^{13}C spins, and the two shoulders at ~19 ppm and ~24 ppm are also now absent, suggesting that they do not arise from the R$_5$ spin system. Next a dipolar recovery at the magic angle (DRAMA) experiment was carried out to exploit the strong couplings within the R5 spin system (normally averaged by sample spinning) in order to selectively eliminate the signals

from the protein by ^{13}C-^{13}C dipolar dephasing. The broad peaks for ([U-^{13}C-R_5]$A\beta_{1-40}$ were virtually abolished, leaving two distinct peaks at the two expected positions for [^{13}C-CH_3]NAcHep (*i.e.*, ~19 ppm and ~24 ppm) (Fig. 6c). Finally a polarization inversion (PI) experiment[27] was used to determine whether the two peaks correspond to methyl groups, as these are present in the saccharide but not in R5 of the peptide. In the PI spectrum, peaks for the methyl and non-protonated carbons remain positive (and well separated in the spectrum), CH_2 peaks are negative and CH peaks are nulled. Here the peaks at ~19 ppm and ~24 ppm remained positive in the spectrum experiment, and so can be positively assigned to CH_3 groups (Fig. 6d). Taken together, this combination of experiments confirms that signals can be detected from [^{13}C-CH_3]NAcHep in the presence of the dominant signals from the peptide. It is therefore possible in principle to detect dipolar couplings between the two species in the aggregates.

The [^{13}C-CH_3]NAcHep/[U-^{13}C-R_5]$A\beta_{1-40}$fibrils were next examined by two dimensional dipolar assisted rotational resonance (DARR) SSNMR[28] to detect protein-glycan interactions. The spectra exhibit several intraresidue cross-peaks and, as the mixing time increases, additional cross-peaks emerge which correlate resonances at ~18–19 ppm and 157 ppm and which are absent from the spectrum of [U-^{13}C-R_5]$A\beta_{1-40}$fibrils alone (Fig. 7). The additional cross-peaks are consistent with weak dipolar coupling between the R_5 guanidinium carbon (Cζ) and the CH_3 group of NAcHep, placing the coupled spins within about 6 Å of each other. Cross-peaks between Cζ and the resonance at 23.5 ppm from [^{13}C-CH_3]NAcHep may also be present but cannot be confirmed because of the dominant resonances for Cβ/Cγ at around 24 ppm. The spectrum nevertheless demonstrates for the first time that intermolecular ^{13}C-^{13}C couplings can be detected between distinct species in heterogeneous amyloid fibrils and indicates that NAcHep and $A\beta_{1-40}$ are in some way mixed at the molecular level to allow the guanidinium carbon (Cζ) of the peptide and the CH_3 group of NAcHep to come into close contact.

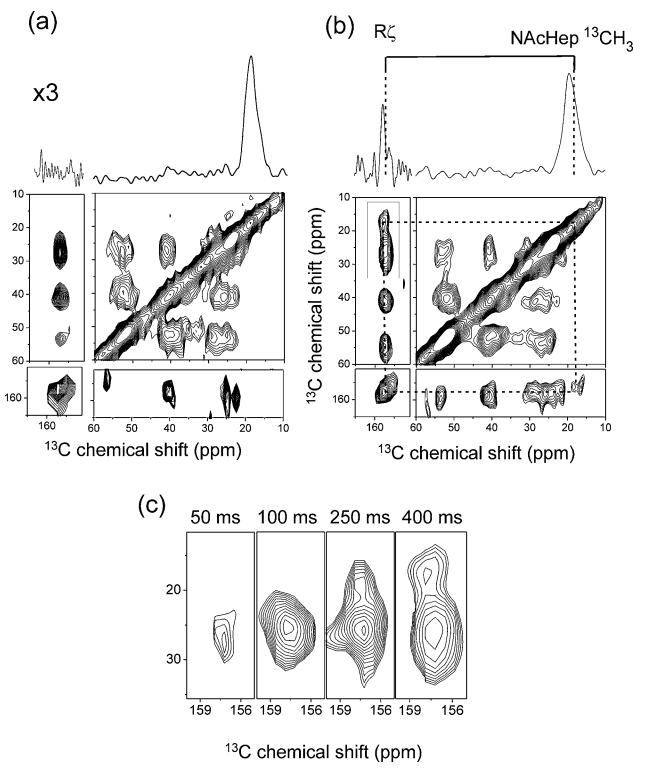

Fig. 7 Detection of peptide-glycan interactions in the fibrils from Fig. 6 using ^{13}C DARR SSNMR. (a) Spectrum of [U-^{13}C-R_5]$A\beta_{1-40}$ fibrils alone. (b) Spectrum of [^{13}C-CH_3]NAcHep/[U-^{13}C-R_5]$A\beta_{1-40}$ fibrils, highlighting cross-peaks between Cζ for R_5 and the methyl ^{13}C of NAcHep. Both spectra were obtained at a mixing time of 400 ms. Shown above each spectrum is a horizontal slice at the frequency of 19 ppm. (c) Cross-peaks between Cζ for R_5 and the methyl ^{13}C of NAcHep at the mixing times shown. The MAS rate and ^1H frequency during the mixing time was 8 kHz. All other conditions are as described in Fig. 5.

This experiment has successfully demonstrated the feasibility of detecting peptide-glycan interactions using SSNMR, but clearly there are currently insufficient constraints to elucidate the precise nature of the interaction and whether R5 plays a specific role in binding GAGs. Indeed, although it is acknowledged that GAGs and other charged species accelerate the aggregation of amyloidogenic proteins and peptides, the degree of specificity of the interaction remains unclear. The saccharide units may simply adorn the surface of the fibrils, or may be intercalated within the protofilament units in a more intricate arrangement. Studies of the effects of various polyelectrolytes including ATP, DNA and heparin with the amyloidogenic proteins acylphosphatase and lysozyme found no evidence for specific interactions, even though the interactions occurred with relatively high affinity.[13]

Conclusions

This work establishes a procedure for detecting GAGs in amyloid aggregates that reflect the composition of amyloid *in vivo*. From DARR SSNMR spectra it has proved possible to identify a population of a ^{13}C labelled HS analogue that is situated close to the N-terminus of the $A\beta_{1-40}$ peptide in amyloid fibrils. Modification of heparin by de-N-sulfation and N-acetylation alters the formal charge of each repeating unit from –4 to –3, but this does not appear to affect significantly the interaction of the analogue with the polypeptide.

Further work is needed to establish whether a specific interaction occurs between NAcHep and $A\beta_{1-40}$, for example by measuring multiple dipolar couplings between the GAG and the putative heparin binding motif V_{12}HHQKL and with amino acid substitutions. By exploiting a novel combination of SSNMR and a ^{13}C-labelled HS proxy, we provide a foundation for extensive SSNMR studies of the interactions between glycans and amyloid proteins in general. The synthetic route to NAcHep is straightforward and also allows for other labelled substituents to be introduced into de-N-sulfated heparin, such as CF_3 or CD_3 acetyl groups. Measurements of heteronuclear (*e.g.* ^{13}C-^{19}F and ^{13}C-^2H) couplings would avoid the problems of overlap encountered here in the ^{13}C SSNMR spectra and could in principle probe longer range intermolecular interactions. This will be important for studies of GAG interaction with uniformly labelled asyn expressed recombinantly. The propensity of amyloidogenic proteins and peptides to form mature fibrils with distinct morphologies suggests that the presence of species such as glycans during the aggregation process could have a profound influence on the molecular structure and morphology of fibrils, the nature of which is not yet clear.

Experimental

Preparation of NAcHep

N-Acetylated heparin bearing a ^{13}C label on the methyl carbon of N-acetyl groups was prepared essentially as described[23] from porcine mucosa intestinal heparin (Celsus, Ohio, USA) *via* selective de-N-sulfation in methanol/DMSO and subsequent selective re N-acetylation of the resulting free amine, employing ^{13}C labelled acetic anhydride (2,2′ $^{13}C_2$; CK Gas Products, Basingstoke, UK).

Preparation of fibrils

The solid $A\beta_{1-40}$ peptide (Peptide Protein Research, UK) was subjected to three dissolution-evaporation cycles with trifluoroacetic acid and a further three cycles with hexafluoroisopropanol to break up any initial aggregates. Fibrils were harvested after incubating 20 μM or 1 mM $A\beta_{1-40}$ in 50 mM phosphate, 100 mM NaCl, pH 7.5, at 37 °C with agitation. In some samples, fibrils were grown in the presence of 1 μM or 1 mM Hep with a mean molecular mass of 16 kDa (Sigma-Aldrich U.K.) or 1 mM NAcHep. Samples were taken for analysis immediately after preparation of the solution and again at specified time points throughout the analysis.

Solid asyn (rPeptide) was subjected to three dissolution-evaporation cycles with trifluoroacetic acid and a further three cycles with hexafluoroisopropanol to break up any initial aggregates. Fibrils were harvested after incubating 20 μM protein in 10 mM Tris, pH7.5, at 37 °C with agitation. Fibrils were grown from protein alone or in the presence of 20 μM Hep or 20 μM NAcHep. Samples were taken for analysis immediately after preparation of the solution and again at specified time points throughout the analysis.

Analysis of aggregation rates and fibril morphology

For monitoring protein aggregation using DLS a series of 20 measurements of 10 seconds each were taken at 30 °C on a Zetasizer Nano instrument from Malvern Instruments and averaged profiles were produced. Aggregation was also monitored with the fluorescent dye ThT. Peptide sample (50 μl) was added to 950 μl of 10 μM ThT (Sigma) in incubation buffer as for protein (50 mM phosphate, 100 mM NaCl, pH 7.5 for Aβ, 10 mM Tris, pH 7.5 for asyn) vortexed and transferred to a 1 cm path length cuvette. Spectra were recorded on a Cary Eclipse Varian fluorescence spectrophotometer with excitation at 450 nm and emission at 482 nm with band pass 5 nm. A new excitation band at 450 nm and enhanced emission at 482 nm are observed when amyloid is present. Morphologies of the insoluble aggregates formed after incubation of Aβ for 24 hours, and asyn for 7 days, were analysed by electron microscopy using negative staining with 2% uranyl acetate. Peptide suspensions (10 μl) were loaded onto carbon coated copper grids and visualised on a Tecnai 10 electron microscope at 100 kV.

NMR

Fibrils were suspended in aqueous buffer, harvested by centrifugation and subjected to 3–4 further resuspension-centrifugation cycles to remove any soluble material. The pellet was transferred to a 4 mm internal diameter zirconium magic-angle spinning rotor for SSNMR and lyophilised *in situ* overnight. All NMR experiments were performed using a Bruker Avance 400 spectrometer operating at a magnetic field of 9.3 Tesla. Experiments were carried out CP-MAS at 25 °C. Experiments utilised an initial 4.0-μs ^1H 90° excitation pulse duration (and a 4.0-μs ^{13}C 90° pulse duration where appropriate), 2 ms Hartmann–Hahn contact time at a ^1H field of 65 kHz, TPPM proton decoupling[29] at a field of 85 kHz during signal acquisition and a 2 s recycle delay. DARR spectra[28] were recorded with 128 hypercomplex points in the indirect dimension (t_1), with a mixing time of 20 ms during which the proton field was adjusted to the spinning frequency of 8 kHz. DQF spectra were obtained with 167 μs C7 double quantum excitation/reconversion.[30] Dipolar dephasing to eliminate signals from the strongly coupled R_5 spin system was achieved using the DRAMA experiment[31] with a mixing period of 17 ms, during which a train of rotationally synchronous 4 μs 180° pulses was applied at the ^{13}C frequency. Samples were rotated at the magic angle at rates of 8 kHz for the DARR experiment and 6 kHz for all other experiments, whilst maintaining the spinning rate automatically to within ±1 Hz.

Acknowledgements

The Alzheimer's Research Trust is acknowledged for a Fellowship to JM. EAY is supported by funding from the BBSRC and DAM is supported by funding from the BBSRC and the British Heart Foundation. The Wellcome Trust is acknowledged for a Value in People award to JCC.

References

1 J. D. Sipe and A. S. Cohen, *J. Struct. Biol.*, 2000, **130**, 88–98.
2 P. Westermark, M. D. Benson, J. N. Buxbaum, A. S. Cohen, B. Frangione, S. I. Ikeda, C. L. Masters, G. Merlini, M. J. Saraiva and J. D. Sipe, *Amyloid-Journal of Protein Folding Disorders*, 2005, **12**, 1–4.
3 M. R. Sawaya, S. Sambashivan, R. Nelson, M. I. Ivanova, S. A. Sievers, M. I. Apostol, M. J. Thompson, M. Balbirnie, J. J. W. Wiltzius, H. T. McFarlane, A. O. Madsen, C. Riekel and D. Eisenberg, *Nature*, 2007, **447**, 453–457.
4 A. T. Petkova, Y. Ishii, J. J. Balbach, O. N. Antzutkin, R. D. Leapman, F. Delaglio and R. Tycko, *Proc. Natl. Acad. Sci. U. S. A.*, 2002, **99**, 16742–16747.
5 H. Heise, *ChemBioChem*, 2008, **9**, 179–189.
6 A. T. Petkova, R. D. Leapman, Z. H. Guo, W. M. Yau, M. P. Mattson and R. Tycko, *Science*, 2005, **307**, 262–265.
7 H. Heise, W. Hoyer, S. Becker, O. C. Andronesi, D. Riedel and M. Baldus, *Proc. Natl. Acad. Sci. U. S. A.*, 2005, **102**, 15871–15876.
8 R. Nelson, M. R. Sawaya, M. Balbirnie, A. O. Madsen, C. Riekel, R. Grothe and D. Eisenberg, *Nature*, 2005, **435**, 773–778.
9 S. Luca, W.-M. Yau, R. D. Leapman and R. Tycko, *Biochemistry*, 2007, **46**, 13505–13522.
10 K. Iwata, T. Fujiwara, Y. Matsuki, H. Akutsu, S. Takahashi, H. Naiki and Y. Goto, *Proc. Natl. Acad. Sci. U. S. A.*, 2006, **103**, 18119–18124.
11 C. P. Jaroniec, C. E. MacPhee, N. S. Astrof, C. M. Dobson and R. G. Griffin, *Proc. Natl. Acad. Sci. U. S. A.*, 2002, **99**, 16748–16753.
12 J. van Horssen, P. Wesseling, L. van den Heuvel, R. M. W. de Waal and M. M. Verbeek, *Lancet Neurology*, 2003, **2**, 482–492.
13 M. Calamai, J. R. Kumita, J. Mifsud, C. Parrini, M. Ramazzotti, G. Ramponi, N. Taddei, F. Chiti and C. M. Dobson, *Biochemistry*, 2006, **45**, 12806–12815.
14 J. A. Cohlberg, J. Li, V. N. Uversky and A. L. Fink, *Biochemistry*, 2002, **41**, 1502–1511.
15 G. M. Castillo, J. A. Cummings, W. H. Yang, M. E. Judge, M. J. Sheardown, K. Rimvall, J. B. Hansen and A. D. Snow, *Diabetes*, 1998, **47**, 612–620.
16 T. Konno, S. Oiki and T. Morii, *FEBS Lett.*, 2007, **581**, 1635–1638.
17 R. Kodali and R. Wetzel, *Curr. Opin. Struct. Biol.*, 2007, **17**, 48–57.

18 B. Klajnert, M. Cortijo-Arellano, M. Bryszewska and J. Cladera, *Biochem. Biophys. Res. Commun.*, 2006, **339**, 577–582.
19 J. Diaz-Nido, F. Wandosell and J. Avila, *Peptides*, 2002, **23**, 1323–1332.
20 G. M. Castillo, W. Lukito, T. N. Wight and A. D. Snow, *J. Neurochem.*, 1999, **72**, 1681–1687.
21 D. J. Watson, A. D. Lander and D. J. Selkoe, *J. Biol. Chem.*, 1997, **272**, 31617–31624.
22 I. H. Liu, V. N. Uversky, L. A. Munishkina, A. L. Fink, W. Halfter and G. J. Cole, *Glycobiology*, 2005, **15**, 1320–1331.
23 Y. Inoue and K. Nagasawa, *Carbohydr. Res.*, 1976, **46**, 87–95.
24 E. A. Yates, F. Santini, M. Guerrini, A. Naggi, G. Torri and B. Casu, *Carbohydr. Res.*, 1996, **294**, 15–27.
25 A. D. Snow, R. Sekiguchi, D. Nochlin, P. Fraser, K. Kimata, A. Mizutani, M. Arai, W. A. Schreier and D. G. Morgan, *Neuron*, 1994, **12**, 219–234.
26 H. Levine, *Protein Sci.*, 1993, **2**, 404–410.
27 X. L. Wu and K. W. Zilm, *J. Magn. Reson., Ser. A*, 1993, **102**, 205–213.
28 K. Takegoshi, S. Nakamura and T. Terao, *Chem. Phys. Lett.*, 2001, **344**, 631–637.
29 A. E. Bennett, C. M. Rienstra, M. Auger, K. V. Lakshmi and R. G. Griffin, *J. Chem. Phys.*, 1995, **103**, 6951.
30 Y. K. Lee, N. D. Kurur, M. Helmle, O. G. Johannessen, N. C. Nielsen and M. H. Levitt, *Chem. Phys. Lett.*, 1995, **242**, 304–309.
31 R. Tycko and G. Dabbagh, *Chem. Phys. Lett.*, 1990, **173**, 461–465.

